Cronfa - Swansea University Open Access Repository

This is an author produced version of a paper published in:
Surface Science Spectra

Cronfa URL for this paper:
http://cronfa.swan.ac.uk/Record/cronfa46101

Paper:

Jones, D., Warwick, M., McGettrick, J. & Dunnill, C. (2018). Composition analysis of $Ta_3N_5/W_{18}O_{49}$ nanocomposite through XPS. *Surface Science Spectra, 25*(2), 024002

http://dx.doi.org/10.1116/1.5047860

Composition analysis of $Ta_3N_5/W_{18}O_{49}$ nanocomposite through XPS

Daniel R. Jones, Michael E. A. Warwick, James D. McGettrick, and Charles W. Dunnill

Citation: Surface Science Spectra **25**, 024002 (2018); doi: 10.1116/1.5047860
View online: https://doi.org/10.1116/1.5047860
View Table of Contents: http://avs.scitation.org/toc/sss/25/2
Published by the American Vacuum Society

Composition analysis of $Ta_3N_5/W_{18}O_{49}$ nanocomposite through XPS

Daniel R. Jones,[1] Michael E. A. Warwick,[1] James D. McGettrick,[2] and Charles W. Dunnill[1,a)]

[1]*Energy Safety Research Institute (ESRI), Swansea University Bay Campus, Swansea SA1 8EN, United Kingdom*

[2]*SPECIFIC Swansea University Bay Campus, Swansea SA1 8EN, United Kingdom*

(Received 10 July 2018; accepted 11 October 2018; published 12 November 2018)

A characterization of a nanocomposite material consisting of Ta_3N_5 nanoparticles and $W_{18}O_{49}$ nanowires is presented. The material is of interest for photocatalytic applications, with a focus on pollution reduction through the photodegradation of dye waste; under white light illumination, the combination of Ta_3N_5 and $W_{18}O_{49}$ yielded an enhanced rate of dye degradation relative to Ta_3N_5 particles alone. The facile method of synthesis is thought to be a promising route for both upscale and commercial utilization of the material. X-ray photoelectron spectroscopy revealed a core–shell composite structure with $W_{18}O_{49}$ present as an overlayer on Ta_3N_5; the analyzed spectra for the C 1*s*, O 1*s*, Ta 4*f*, N 1*s*, W 4*f*, and Na 1*s* regions are reported. It should be noted that due to differential charging of the underlying Ta_3N_5 component relative to the $W_{18}O_{49}$ shell, an additional uncompensated voltage shift may exist in the Ta 4*f* and N 1*s* spectra. *Published by the AVS.*

https://doi.org/10.1116/1.5047860

Keywords: *Ta_3N_5, $W_{18}O_{49}$, photocatalysis, dye degradation, composite, nanowires, x-ray photoelectron spectroscopy, XPS*

Accession #: 01477

Technique: XPS

Host Material: $Ta_3N_5/W_{18}O_{49}$ nanocomposite

Instrument: Kratos Axis Supra

Major Elements in Spectra: W, O

Minor Elements in Spectra: Ta, N, C

Published Spectra: 6

Spectra in Electronic Record: 6

Spectral Category: Comparison

INTRODUCTION

Many synthetic dyes are toxic to both human (Ref. 1) and marine life (Ref. 2) and inhibit aquatic photosynthesis through light absorption (Ref. 3), leading to concerns for global oxygen production. Many synthetic dyes are, by design, chemically stable and are therefore difficult to degrade via common biological treatment (Refs. 4 and 5), while alternative techniques can lead to the production of unwanted by-products which are also harmful (Refs. 6–9). One promising, low-energy solution for the remediation of dye-polluted water is the use of photocatalysts for oxidation of the dyes. Much work has focused on the use of TiO_2 nanopowders for this purpose (Refs. 10–17); however, TiO_2 has a wide bandgap (3.2 eV) and can therefore utilize only the ultraviolet portion of the solar spectrum, which accounts for a small percentage of solar radiation that reaches the earth. With this in mind, it is preferable to employ a material with a narrower bandgap so that dye oxidation may be instigated by visible light. With its low bandgap of 2.1 eV (Ref. 18), Ta_3N_5 has been shown to work well as a visible light photocatalyst for the degradation of organic dyes (Refs. 19–21), although our recent study demonstrated how the catalytic performance of this material may be enhanced through a strategic combination with tungsten(IV) suboxide nanowires in the form of a composite (Ref. 22). Within this investigation, a solvothermal approach was employed to grow $W_{18}O_{49}$ nanofibers on Ta_3N_5 nanoparticles inside a polytetrafluoroethylene-lined stainless steel acid digestion bomb, and it was found that the combination of these materials resulted in improved charge carrier separation due to electron–hole transfer at the interface of the two components; the increase in charge separation afforded longer charge carrier lifetimes, resulting in a marked increase in the photocatalytic activity of the material. To the best of the authors' knowledge, this system has not before been synthesized for the purpose of water remediation.

SPECIMEN DESCRIPTION (ACCESSION #01477)

Host Material: $Ta_3N_5/W_{18}O_{49}$ nanocomposite

CAS Registry #: Unknown

Host Material Characteristics: Inhomogeneous; powder; polycrystalline; semiconductor; composite

Chemical Name: Tantalum(V) nitride/tungsten(VI) suboxide

Source: Solvothermally grown $W_{18}O_{49}$ on Ta_3N_5 from ammonolyzed $TaCl_5$

Host Composition: $Ta_3N_5/W_{18}O_{49}$

Form: Polycrystalline composite

Structure: Orthorhombic Ta_3N_5/monoclinic $W_{18}O_{49}$

History and Significance: Ta_3N_5 nanoparticles were prepared through ammonolysis of $TaCl_5$ powder in a 7:3 molar ratio of KCl and NaCl at 800 °C for 10 h. Nanowires of $W_{18}O_{49}$ were subsequently grown solvothermally on the surface of the Ta_3N_5 nanoparticles by annealing a suspension of the nanoparticles in a solution of WCl_6 in a 4:1 volumetric mixture of ethanol and ethylene glycol at 180 °C for 24 h, followed by centrifugation of the product in ethanol and deionized water.

As Received Condition: The as-synthesized composite had the form of a brown powder.

Analyzed Region: Same as the host material

***Ex Situ* Preparation/Mounting:** The composite powder was loaded into a 5 mm pellet press and pelletized using a force of 2 tons. The pellet was retrieved from the press and mounted on an adhesive carbon tab for analysis.

***In Situ* Preparation:** None

a)Electronic mail: c.dunnill@swansea.ac.uk

Charge Control: Electronic charge neutralization using magnetic immersion lens. Filament current = 0.4 A, charge balance = 3.3 V, filament bias = 1.0 V.

Temp. During Analysis: 300 K

Pressure During Analysis: 4×10^{-6} Pa

Preanalysis Beam Exposure: 0 s

INSTRUMENT DESCRIPTION

Manufacturer and Model: Kratos Axis Supra

Analyzer Type: Spherical sector

Detector: Multichannel resistive plate

Number of Detector Elements: 3 MCP, 128 channel DLD

INSTRUMENT PARAMETERS COMMON TO ALL SPECTRA

■ *Spectrometer*

Analyzer Mode: Constant pass energy

Throughput ($T = E^N$): N = 0

Excitation Source Window: Not specified

Excitation Source: Al K_α monochromatic

Source Energy: 1486.6 eV

Source Strength: 225 W

Source Beam Size: 700 μm $\times$ 300 μm

Signal Mode: Multichannel direct

■ *Geometry*

Incident Angle: 54.7°

Source-to-Analyzer Angle: 54.7°

Emission Angle: 0°

Specimen Azimuthal Angle: N/A

Acceptance Angle from Analyzer Axis: 0°

Analyzer Angular Acceptance Width: 30° × 30°

■ *Ion Gun*

Manufacturer and Model: Kratos GCIS Minibeam 6

Energy: 10 keV

Current: 23 nA

Current Measurement Method: Biased stage

Sputtering Species: Argon 1000+ ion clusters

Spot Size (unrastered): 200 μm

Raster Size: 2000 μm $\times$ 2000 μm

Incident Angle: 40°

Polar Angle: 0°

Azimuthal Angle: 0°

Comment: Sputtering was carried out on the reference samples only.

DATA ANALYSIS METHOD

Energy Scale Correction: The binding energy scale was referenced to C 1*s* = 284.8 eV.

Recommended Energy Scale Shift: 3.213 eV

Peak Shape and Background Method: Peak shape: Gaussian–Lorentzian product formula GL(30). Background: The Shirley background was used.

Quantitation Method: Quantification was achieved through peak deconvolution using CASAXPS version 2.3.15. Relative sensitivity factors were supplied by Kratos Analytical.

ACKNOWLEDGMENTS

Financial support was provided by the Welsh Government Sêr Cymru Programme and the Flexis project, which is part-funded by the European Regional Development Fund (ERDF) through the Welsh Government.

REFERENCES

1. T. Plaztek, C. Lang, G. Grohmann, U.-S. Gi, and W. Baltes, Hum. Exp. Toxicol. **18**, 552 (1999).
2. M. Sumathi, K. Kalaiselvi, M. Palanivel, and P. Rajaguru, Bull. Environ. Contam. Toxicol. **66**, 407 (2001).
3. O. Gulnaz, J. Hazard. Mater. **108**, 183 (2004).
4. A. Srinivasan and T. Viraraghavan, J. Environ. Manage. **91**, 1915 (2010).
5. T. Robinson, G. McMullan, R. Marchant, and P. Nigam, Bioresour. Technol. **77**, 247 (2001).
6. H. Nourmoradi, S. Zabihollahi, and H. R. Pourzamani, Desalin. Water Treat. **57**, 5200 (2015).
7. A. K. Verma, R. R. Dash, and P. Bhunia, J. Environ. Manage. **93**, 154 (2012).
8. Y. Li *et al.*, Chem. Eng. Res. Des. **91**, 361 (2013).
9. G. Mezohegyi, F. P. van der Zee, J. Font, A. Fortuny, and A. Fabregat, J. Environ. Manage. **102**, 148 (2012).
10. A. Ajmal, I. Majeed, R. N. Malik, H. Idriss, and M. A. Nadeem, RSC Adv. **4**, 37003 (2014).
11. J. C. Bear, V. Gomez, N. S. Kefallinos, J. D. McGettrick, A. R. Barron, and C. W. Dunnill, J. Colloid Interf. Sci. **460**, 29 (2015).
12. V. Gomez, J. C. Bear, P. D. McNaughter, J. D. McGettrick, T. Watson, C. Charbonneau, P. O'Brien, A. R. Barron, and C. W. Dunnill, Nanoscale **7**, 17735 (2015).
13. C. W. Dunnill, Z. A. Aiken, J. Pratten, M. Wilson, and I. P. Parkin, Chem. Vap. Deposition **16**, 50 (2010).
14. C. W. Dunnill, Z. Ansari, A. Kafizas, S. Perni, D. J. Morgan, M. Wilson, and I. P. Parkin, J. Mater. Chem. **21**, 11854 (2011).
15. C. W. Dunnill, S. Noimark, and I. P. Parkin, Thin Solid Films **520**, 5516 (2012).
16. M. E. A. Warwick, C. W. Dunnill, and R. Binions, Chem. Vap. Deposition **16**, 220 (2010).
17. C. W. Dunnill, K. Page, Z. A. Aiken, S. Noimark, G. Hyett, A. Kafizas, J. Pratten, M. Wilson, and I. P. Parkin, J. Photochem. Photobiol. A **220**, 113 (2011).
18. M. Hara, G. Hitoki, T. Takata, J. N. Kondo, H. Kobayashi, and K. Domen, Catal. Today **78**, 555 (2003).
19. Z. Wang, J. Hou, S. Jiao, K. Huang, and H. Zhu, J. Mater. Chem. **22**, 21972 (2012).
20. D.-H. Lin and K.-S. Chang, J. Appl. Phys. **120**, 075303 (2016).
21. S.-T. Bae, H. Shin, S. Lee, D. W. Kim, H. S. Jung, and K. S. Hong, React. Kinet. Mech. Cat. **106**, 67 (2011).
22. D. R. Jones *et al.*, Sci. Rep. **7**, 4090 (2017).

SPECTRAL FEATURES TABLE							
Spectrum ID #	**Element/ Transition**	**Peak Energy (eV)**	**Peak Width FWHM (eV)**	**Peak Area (eV × counts/s)**	**Sensitivity Factor**	**Concentration (at. %)**	**Peak Assignment**
01477-02	W $4f_{7/2}$	35.9	1.14	33 987	3.523	12.84	WO_3
01477-02	W $4f_{5/2}$	38.1	1.14	25 490	3.523	…	WO_3
01477-02	W $4f_{7/2}$	34.6	0.93	4 298	3.523	…	W_2O_5
01477-02	W $4f_{5/2}$	36.7	0.93	3 223	3.523	…	W_2O_5
01477-03	O 1*s*	530.6	1.21	41 006	0.780	40.20	WO_3/W_2O_5
01477-03	O 1*s*	531.6	1.21	8 556	0.780	…	Surface –OH
01477-03	O 1*s*	532.6	1.21	5 319	0.780	…	Adventitious organics
01477-03	O 1*s*	533.6	1.21	2 904	0.780	…	Adventitious organics
01477-04	C 1*s*	284.8	1.35	18 539	0.278	45.52	Adventitious C–C/C–H
01477-04	C 1*s*	286.4	1.35	2 820	0.278	…	Adventitious C–O/C=O
01477-05	Ta 4*f*	25.4	0.86	1 731	3.082	0.62	Ta_3N_5
01477-06	N 1*s*	396.7	0.93	351	0.477	0.81	Ta_3N_5

ANALYZER CALIBRATION TABLE							
Spectrum ID #	**Element/ Transition**	**Peak Energy (eV)**	**Peak Width FWHM (eV)**	**Peak Area (eV × counts/s)**	**Sensitivity Factor**	**Concentration (at. %)**	**Peak Assignment**
08	Ag $3d_{5/2}$	368.4	0.51	71 961	5.987	…	Ag
10	Au $4f_{7/2}$	84.0	0.60	314 838	6.250	…	Au
12	Cu $2p_{3/2}$	933.0	0.80	401 503	5.321	…	Cu

GUIDE TO FIGURES					
Spectrum (Accession) #	Spectral Region	Voltage Shift[a]	Multiplier	Baseline	Comment #[b]
01477-01	Survey	3.213	1	0	1
01477-02	W 4*f*	3.213	1	0	1
01477-02	W 4*f*	3.213	1	0	1
01477-03	O 1*s*	3.213	1	0	1
01477-03	O 1*s*	3.213	1	0	1
01477-04	C 1*s*	3.213	1	0	1
01477-04	C 1*s*	3.213	1	0	1
01477-05	Ta 4*f*	3.213	1	0	1
01477-06	N 1*s*	3.213	1	0	1
07	Survey	0	1	0	2
08	Ag $3d_{5/2}$	0	1	0	2
09	Survey	0	1	0	3
10	Au $4f_{7/2}$	0	1	0	3
11	Survey	0	1	0	4
12	Cu $2p_{3/2}$	0	1	0	4

[a]Voltage shift of the published figure relative to the as-measured spectrum; the energy correction accounts for the effects of sample charging.
[b]1. $Ta_3N_5/W_{18}O_{49}$ nanocomposite. 2. Ag calibration. 3. Au calibration. 4. Cu calibration.

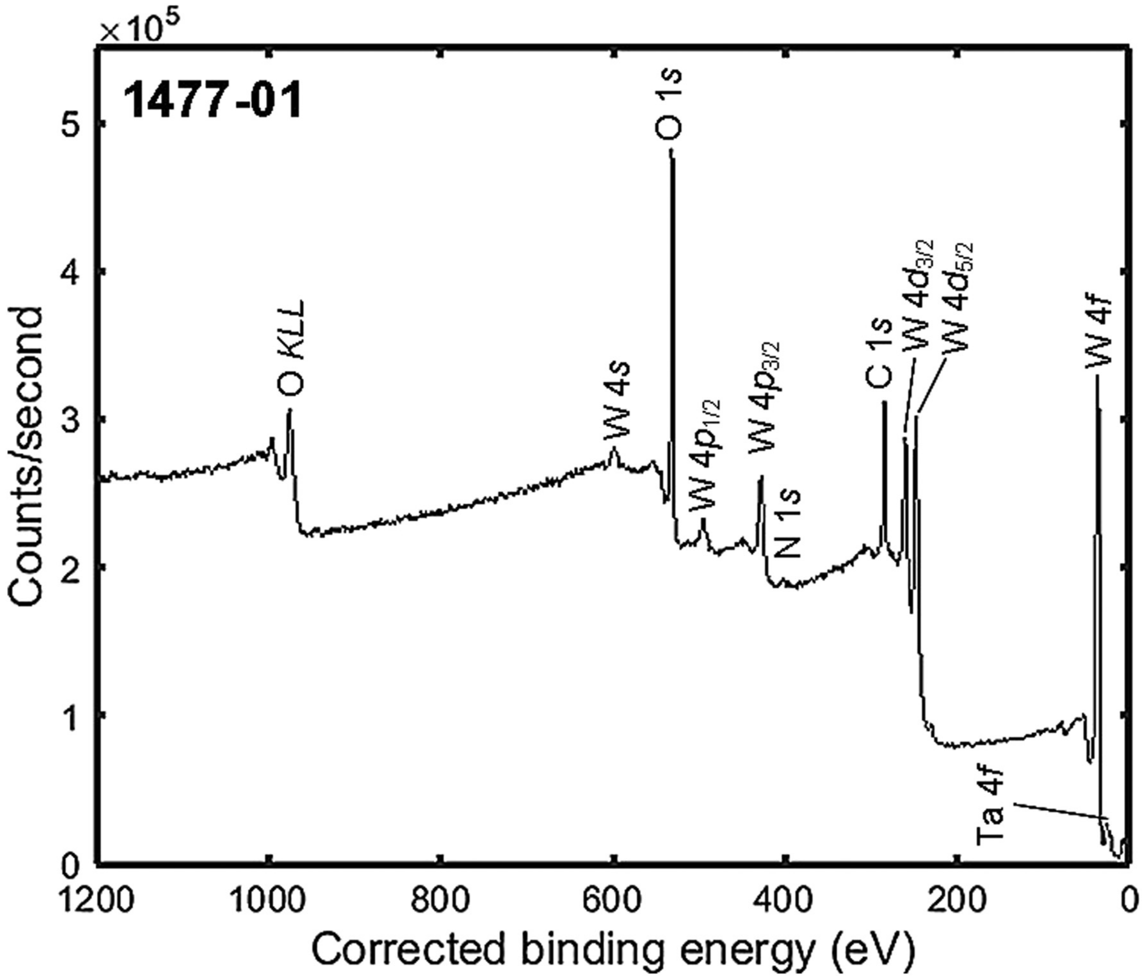

Accession #	01477-01
Host Material:	$Ta_3N_5/W_{18}O_{49}$ nanocomposite
Technique:	XPS
Spectral Region:	Survey
Instrument:	Kratos Axis Supra
Excitation Source:	Al K_α monochromatic
Source Energy:	1486.6 eV
Source Strength:	225 W
Source Size:	0.7 mm × 0.3 mm
Analyzer Type:	Spherical sector analyzer
Incident Angle:	54.7°
Emission Angle:	0°
Analyzer Pass Energy:	160 eV
Analyzer Resolution:	1 eV
Total Signal Accumulation Time:	120 s
Total Elapsed Time:	Not specified
Number of Scans:	1
Effective Detector Width:	16 eV

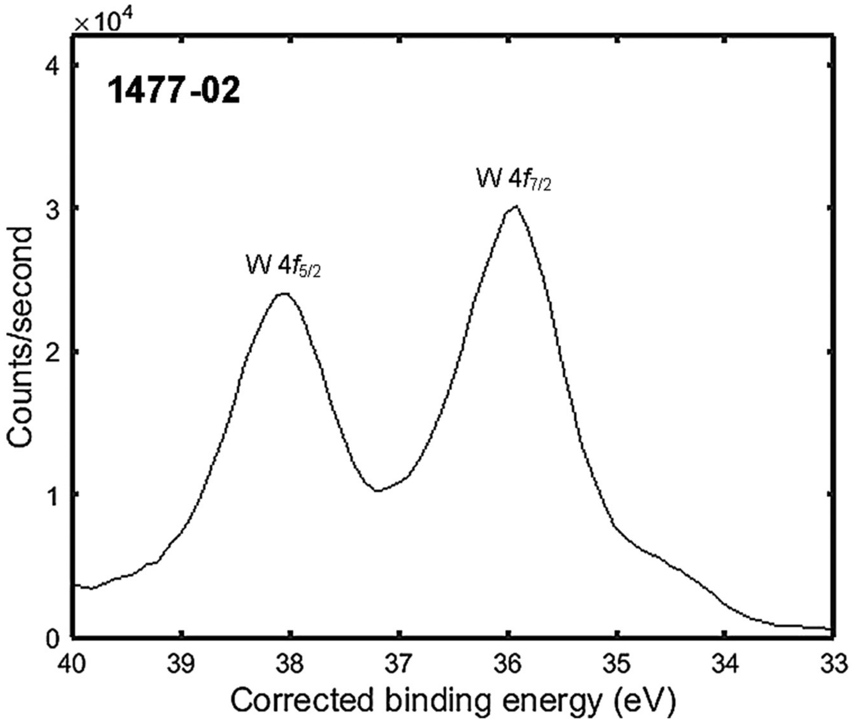

- **Accession #:** 01477-02
- **Host Material:** Ta_3N_5/ $W_{18}O_{49}$ nanocomposite
- **Technique:** XPS
- **Spectral Region:** W 4*f*

Instrument: Kratos Axis Supra

Excitation Source: Al K_{α} monochromatic

Source Energy: 1486.6 eV

Source Strength: 225 W

Source Size: 0.7 mm × 0.3 mm

Analyzer Type: Spherical sector

Incident Angle: 54.7°

Emission Angle: 0°

Analyzer Pass Energy: 20 eV

Analyzer Resolution: 0.1 eV

Total Signal Accumulation Time: 17.75 s

Total Elapsed Time: Not specified

Number of Scans: 1

Effective Detector Width: 2 eV

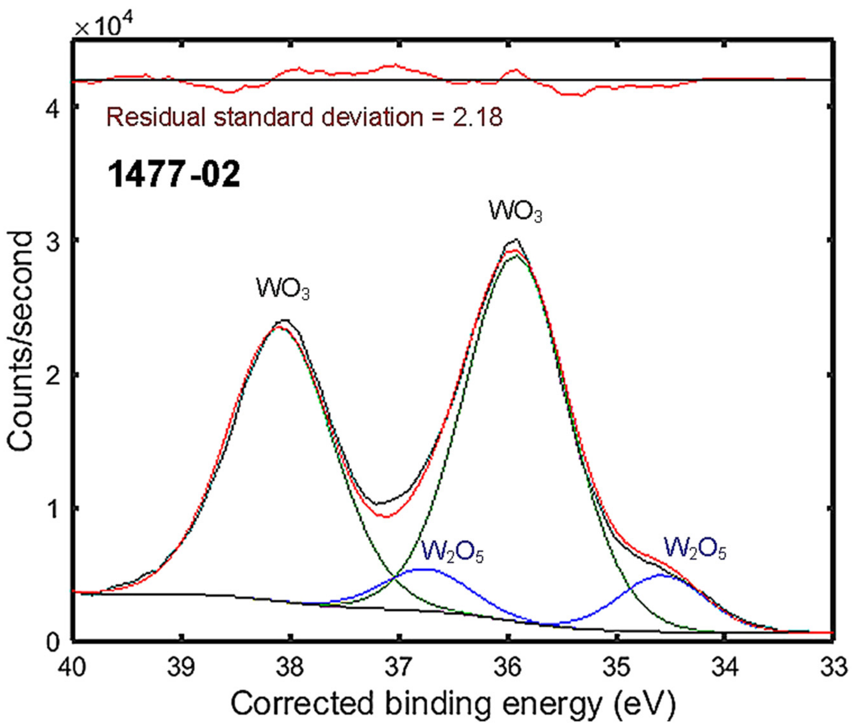

- **Accession #:** 01477-02
- **Host Material:** Ta_3N_5/ $W_{18}O_{49}$ nanocomposite
- **Technique:** XPS
- **Spectral Region:** W 4*f*

Instrument: Kratos Axis Supra

Excitation Source: Al K_{α} monochromatic

Source Energy: 1486.6 eV

Source Strength: 225 W

Source Size: 0.7 mm × 0.3 mm

Analyzer Type: Spherical sector

Incident Angle: 54.7°

Emission Angle: 0°

Analyzer Pass Energy: 20 eV

Analyzer Resolution: 0.1 eV

Total Signal Accumulation Time: 17.75 s

Total Elapsed Time: Not specified

Number of Scans: 1

Effective Detector Width: 2 eV

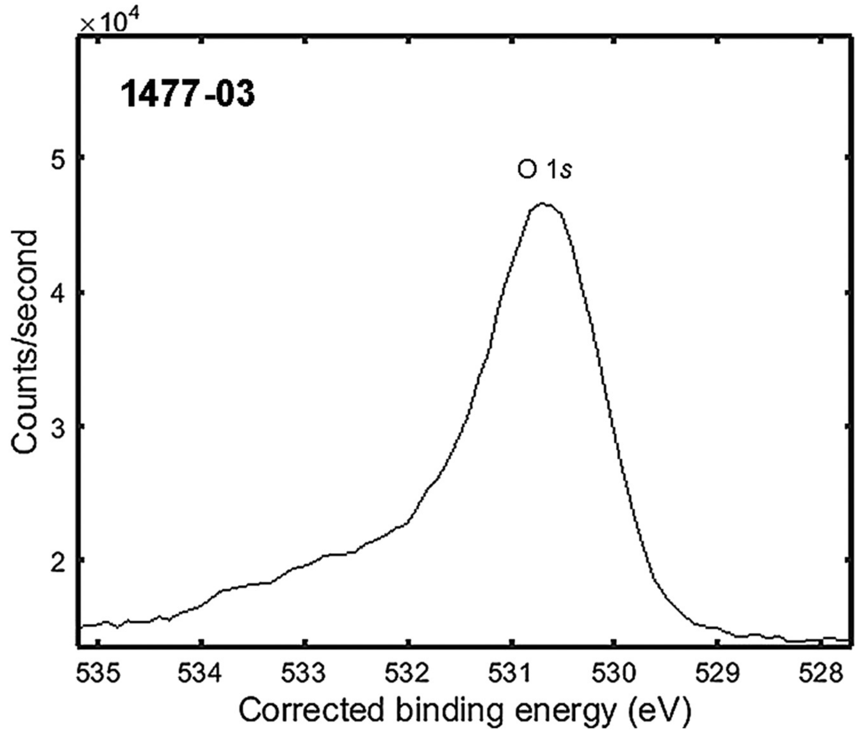

- **Accession #:** 01477-03
- **Host Material:** Ta_3N_5/ $W_{18}O_{49}$ nanocomposite
- **Technique:** XPS
- **Spectral Region:** O 1*s*

Instrument: Kratos Axis Supra

Excitation Source: Al K_α monochromatic

Source Energy: 1486.6 eV

Source Strength: 225 W

Source Size: 0.7 mm × 0.3 mm

Analyzer Type: Spherical sector

Incident Angle: 54.7°

Emission Angle: 0°

Analyzer Pass Energy: 20 eV

Analyzer Resolution: 0.1 eV

Total Signal Accumulation Time: 19 s

Total Elapsed Time: Not specified

Number of Scans: 1

Effective Detector Width: 2 eV

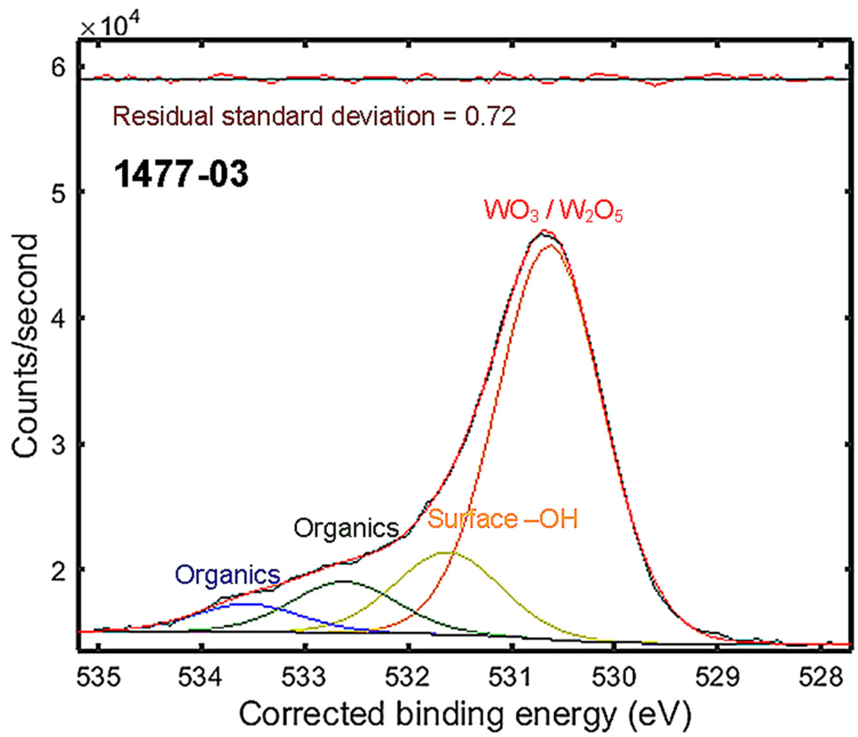

- **Accession #:** 01477-03
- **Host Material:** Ta_3N_5/ $W_{18}O_{49}$ nanocomposite
- **Technique:** XPS
- **Spectral Region:** O 1*s*

Instrument: Kratos Axis Supra

Excitation Source: Al K_α monochromatic

Source Energy: 1486.6 eV

Source Strength: 225 W

Source Size: 0.7 mm × 0.3 mm

Analyzer Type: Spherical sector

Incident Angle: 54.7°

Emission Angle: 0°

Analyzer Pass Energy: 20 eV

Analyzer Resolution: 0.1 eV

Total Signal Accumulation Time: 19 s

Total Elapsed Time: Not specified

Number of Scans: 1

Effective Detector Width: 2 eV

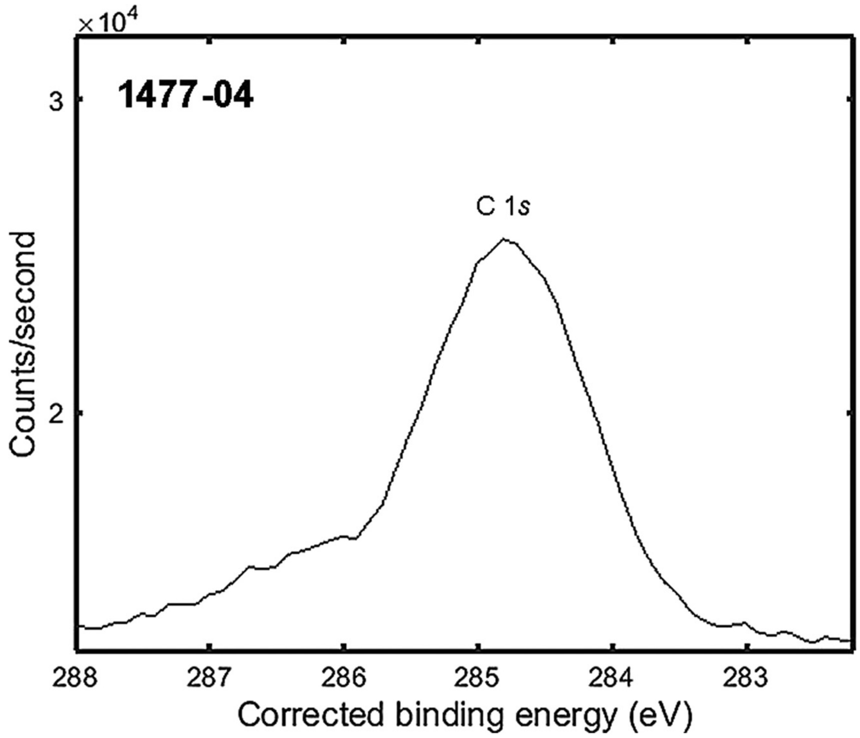

- **Accession #:** 01477-04
- **Host Material:** Ta_3N_5/$W_{18}O_{49}$ nanocomposite
- **Technique:** XPS
- **Spectral Region:** C 1*s*

Instrument: Kratos Axis Supra

Excitation Source: Al K_α monochromatic

Source Energy: 1486.6 eV

Source Strength: 225 W

Source Size: 0.7 mm × 0.3 mm

Analyzer Type: Spherical sector

Incident Angle: 54.7°

Emission Angle: 0°

Analyzer Pass Energy: 20 eV

Analyzer Resolution: 0.1 eV

Total Signal Accumulation Time: 29.5 s

Total Elapsed Time: Not specified

Number of Scans: 2

Effective Detector Width: 2 eV

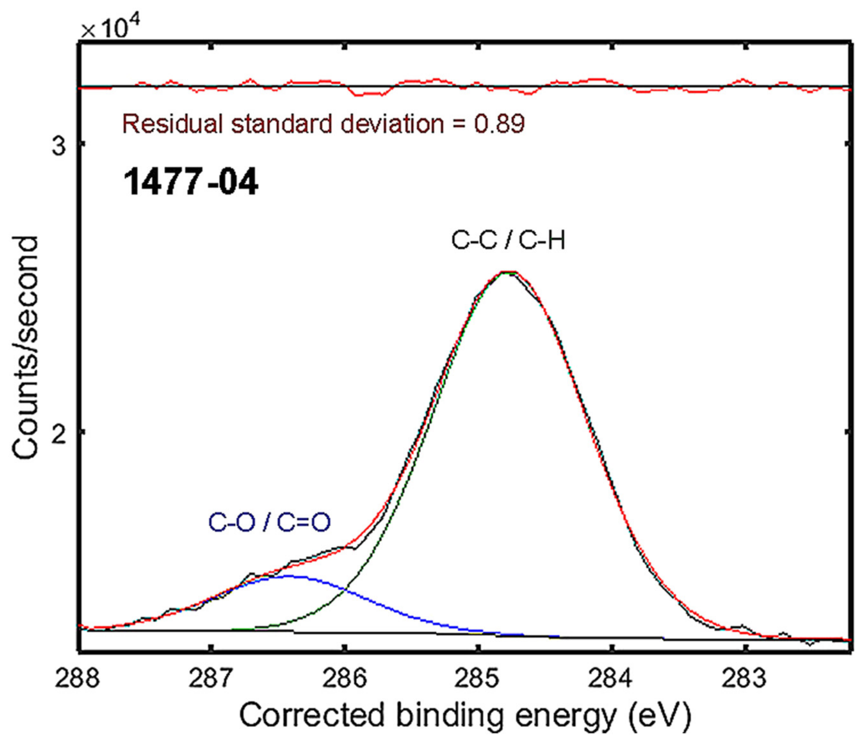

- **Accession #:** 01477-04
- **Host Material:** Ta_3N_5/$W_{18}O_{49}$ nanocomposite
- **Technique:** XPS
- **Spectral Region:** C 1*s*

Instrument: Kratos Axis Supra

Excitation Source: Al K_α monochromatic

Source Energy: 1486.6 eV

Source Strength: 225 W

Source Size: 0.7 mm × 0.3 mm

Analyzer Type: Spherical sector

Incident Angle: 54.7°

Emission Angle: 0°

Analyzer Pass Energy: 20 eV

Analyzer Resolution: 0.1 eV

Total Signal Accumulation Time: 29.5 s

Total Elapsed Time: Not specified

Number of Scans: 2

Effective Detector Width: 2 eV

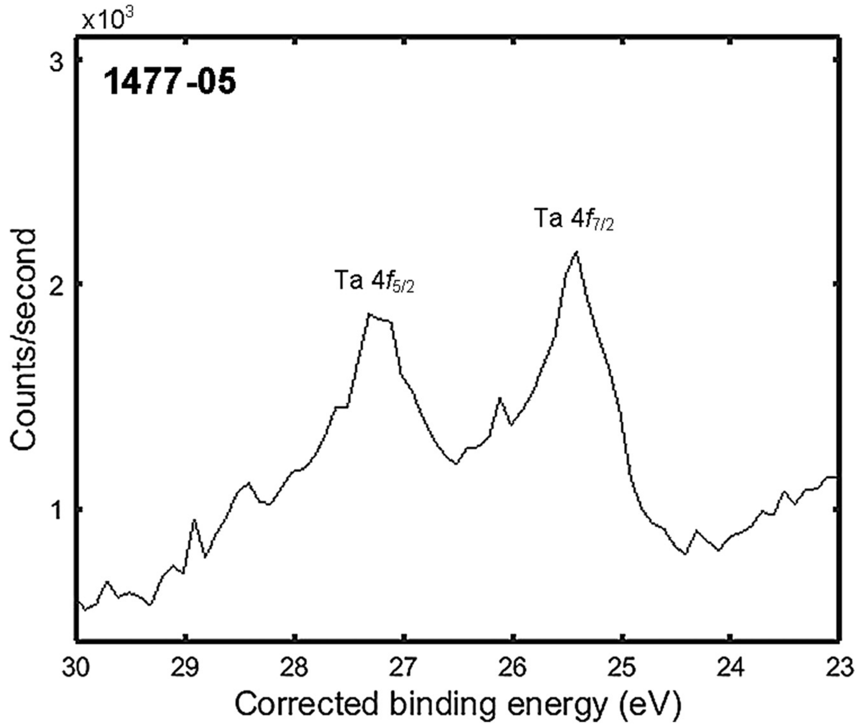

- **Accession #:** 01477-05
- **Host Material:** Ta_3N_5/ $W_{18}O_{49}$ nanocomposite
- **Technique:** XPS
- **Spectral Region:** Ta 4*f*

Instrument: Kratos Axis Supra

Excitation Source: Al K_α monochromatic

Source Energy: 1486.6 eV

Source Strength: 225 W

Source Size: 0.7 mm × 0.3 mm

Analyzer Type: Spherical sector

Incident Angle: 54.7°

Emission Angle: 0°

Analyzer Pass Energy: 20 eV

Analyzer Resolution: 0.1 eV

Total Signal Accumulation Time: 17.5 s

Total Elapsed Time: Not specified

Number of Scans: 1

Effective Detector Width: 2 eV

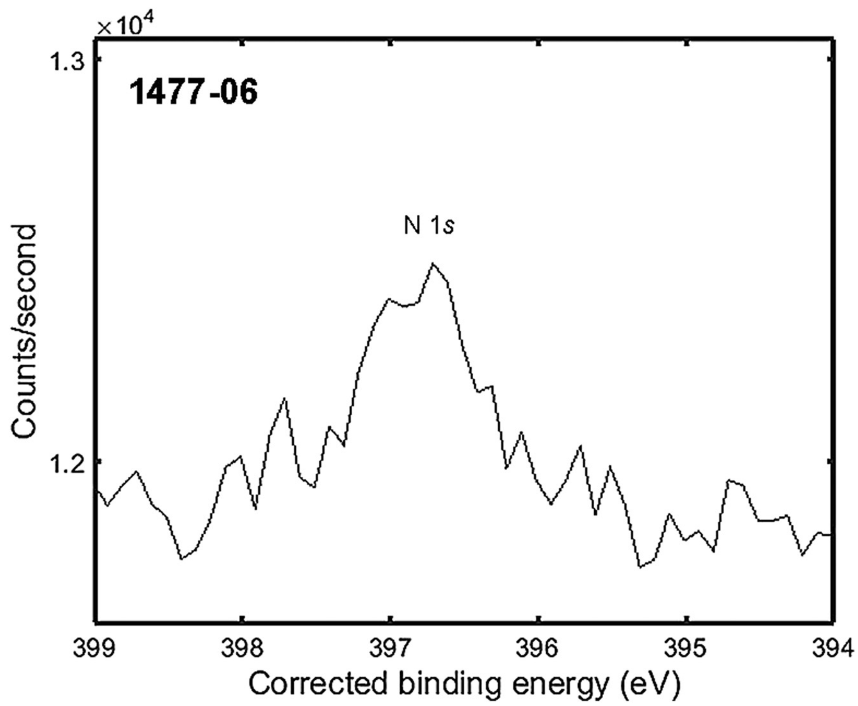

- **Accession #:** 01477-06
- **Host Material:** Ta_3N_5/ $W_{18}O_{49}$ nanocomposite
- **Technique:** XPS
- **Spectral Region:** N 1*s*

Instrument: Kratos Axis Supra

Excitation Source: Al K_α monochromatic

Source Energy: 1486.6 eV

Source Strength: 225 W

Source Size: 0.7 mm × 0.3 mm

Analyzer Type: Spherical sector

Incident Angle: 54.7°

Emission Angle: 0°

Analyzer Pass Energy: 20 eV

Analyzer Resolution: 0.1 eV

Total Signal Accumulation Time: 62.5 s

Total Elapsed Time: Not specified

Number of Scans: 5

Effective Detector Width: 2 eV